Neuron
Article

A Yeast Genetic Screen Reveals a Critical Role for the Pore Helix Domain in TRP Channel Gating

Benjamin R. Myers,[1] Christopher J. Bohlen,[1] and David Julius[1,*]
[1]Department of Physiology, University of California, San Francisco, 600 16th Street, San Francisco, CA 94143-2140, USA
*Correspondence: julius@cmp.ucsf.edu
DOI 10.1016/j.neuron.2008.04.012

SUMMARY

TRP cation channels function as cellular sensors in uni- and multicellular eukaryotes. Despite intensive study, the mechanisms of TRP channel activation by chemical or physical stimuli remain poorly understood. To identify amino acid residues crucial for TRP channel gating, we developed an unbiased, high-throughput genetic screen in yeast that uncovered rare, constitutively active mutants of the capsaicin receptor, TRPV1. We show that mutations within the pore helix domain dramatically increase basal channel activity and responsiveness to chemical and thermal stimuli. Mutation of corresponding residues within two related TRPV channels leads to comparable effects on their activation properties. Our data suggest that conformational changes in the outer pore region are critical for determining the balance between open and closed states, providing evidence for a general role for this domain in TRP channel activation.

INTRODUCTION

Members of the transient receptor potential (TRP) family of nonselective cation channels participate in a wide variety of physiological processes in organisms ranging from fungi to humans (Clapham, 2003; Dhaka et al., 2006). TRP channels respond to such diverse agonists as hypertonicity in yeast, light-evoked phospholipase C (PLC) activation in the *Drosophila* photoreceptor, and noxious chemical and thermal stimuli in the mammalian somatosensory system. Accordingly, spontaneous loss- and gain-of-function mutations in TRP channels underlie disease states resulting from decreased or increased cation influx, respectively (Nilius, 2007). TRP channels belong to the six-transmembrane-domain (6TM, S1–S6) cation channel superfamily that includes depolarization-activated K^+, Na^+, and Ca^{2+} channels, as well as cyclic-nucleotide-gated (CNG) and hyperpolarization-activated (HCN) channels. TRP channels fall into several subfamilies, including vanilloid (V), canonical (C), and melastatin (M) groups, with most members suspected to form tetramers in vivo. Based on hydropathy predictions, each subunit contains intracellular N and C termini and a membrane-reentrant pore loop between S5 and S6. As a class, TRP channels bear resemblance at the level of transmembrane topology but show remarkably little primary sequence homology within and across subfamilies (Clapham, 2003).

TRP channels respond to an array of stimuli, including physical and chemical agonists (Clapham, 2003; Dhaka et al., 2006). For example, TRPV1, the founding member of the vanilloid subfamily, is the receptor for capsaicin (the pungent ingredient in "hot" chili peppers) but also responds to extracellular protons, bioactive lipids, and noxious heat (>43°C) (Caterina et al., 1997; Jordt et al., 2003; Tominaga et al., 1998). Like many other members of the TRP channel family, TRPV1 can also be modulated by PLC-coupled signal transduction pathways (Chuang et al., 2001; Lukacs et al., 2007; Prescott and Julius, 2003). However, the molecular mechanisms underlying TRP channel activation, ranging from stimulus detection to the regulation of channel opening (gating), are poorly understood. This stands in contrast to other 6TM channels, most notably voltage-activated K^+ channels, which have been probed in great detail using biophysical and crystallographic methods (Tombola et al., 2006; Yellen, 1998).

For voltage-gated channels, an important clue to their common activation mechanism came from visual inspection of linear protein sequences, which revealed a discrete domain (the positively charged S4 helix) as a likely universal candidate for translating changes in plasma membrane voltage into channel opening (Tombola et al., 2006; Yellen, 1998). In contrast, TRP channels are activated by a diversity of chemical and physical stimuli for which corresponding functional motifs are not readily apparent in the channel polypeptide (Clapham, 2003), making it challenging to gain insight into the gating process. Furthermore, TRP and voltage-gated channels are not only functionally divergent but also show sparingly little sequence similarity. Thus, the use of previously developed structural and mechanistic models to ascertain TRP channel function is rather limited. This leaves unanswered the important question of whether any unifying mechanistic principles underlie TRP channel gating.

While previous reports have delineated molecular determinants for agonist binding and activation in several TRP family members, including TRPV1 (Jordt and Julius, 2002; Jordt et al., 2000; Jung et al., 2002), few if any conserved structural elements controlling TRP channel gating have been reported. The difficulty in pinpointing critical gating domains stems, in part, from the challenge of conducting mutational analyses that efficiently sample a large sequence space. Conventional ion channel structure-function studies generally entail the construction and testing of channel mutants one at a time; such studies are low throughput, precluding an unbiased examination in which multiple substitutions at each sequence position are evaluated for functional alterations. Some studies have exploited amino acid polymorphisms between functionally divergent TRP channel family members to narrow down blocks of sequence

that contain determinants of agonist activation (via analysis of chimeric channels) (Chuang et al., 2004; Jordt and Julius, 2002), but this methodology is poorly suited to uncovering core structural elements that are expected to show high levels of conservation among TRP channels. Such limitations can be partially overcome by using robotic methods to sample large numbers of individual mutants via high-throughput functional assays (Bandell et al., 2006; Decaillot et al., 2003; Zhou et al., 2007). Alternatively, genetic strategies based on simple life-or-death readouts (Loukin et al., 1997; Minor et al., 1999; Ou et al., 1998) could permit selection of functionally interesting channel mutants, but such a methodology has not been applied to mammalian TRP channels.

Here, we describe the identification and characterization of a critical component of the TRP channel gating machinery via unbiased genetic screening of a randomly generated population of TRPV1 mutants. We conducted this high-throughput screen on mammalian TRPV1 heterologously expressed in the budding yeast *Saccharomyces cerevisiae*, whose superior genetics allows for the efficient isolation of constitutively active channel alleles. Our study reveals that gain-of-function substitutions in the pore helix of TRPV1 dramatically affect channel activation, establishing an important role for this domain in TRPV1 functionality. We extend these observations to two other members of the TRPV subfamily, suggesting that the pore helix is a key regulatory domain that plays a conserved role in the gating of at least a subset of excitatory TRP channels.

RESULTS

Functional Expression of the Capsaicin Receptor in Yeast

Persistent activation of native or recombinant vanilloid receptors leads to a dramatic decrease in mammalian cell viability due to overload with cations (Caterina et al., 1997; Jancso et al., 1977; Wood et al., 1988). We reasoned that if TRPV1 forms functional channels upon heterologous expression in yeast, then exposure to capsaicin should be fatal. Indeed, yeast transformed with TRPV1 grew robustly on standard solid medium but failed to grow on medium containing capsaicin (Figure 1A). Capsaicin-evoked toxicity was concentration dependent with half-maximal death occurring in the high nanomolar range (data not shown), consistent with established dose-response profiles in mammalian cells (Gunthorpe et al., 2000; Jerman et al., 2000; Oh et al., 1996). In contrast, capsaicin did not change the viability of a strain harboring a Kir2.1 inward rectifier K^+ channel (Minor et al., 1999) (Figure 1A), suggesting that capsaicin-evoked toxicity is mediated by TRPV1 and is not simply an artifact of expressing a foreign cation channel. Along these lines, we found that lethality was fully suppressed by a TRPV1 pore blocker, ruthenium red (10 μM) (Figure 1A), or significantly attenuated by an inverse agonist, capsazepine (50 μM) (data not shown). We have previously described a hypersensitive TRPV1 mutant in which an inhibitory C-terminal putative PIP_2 binding module has been deleted, leading to activation at subthreshold agonist concentrations or ambient temperatures (Prescott and Julius, 2003). Consistent with such functional properties, we found that expression of this potentiated mutant (TRPV1 Δ777-820) was lethal to yeast even in the absence of capsaicin, but growth was restored to wild-type levels in the presence of ruthenium red (Figure 1B). Furthermore, we found that the lethality of capsaicin was augmented when the yeast medium was supplemented with higher levels of sodium (data not shown), suggesting that, as in mammalian cells, toxicity stems from a rise in intracellular cation concentrations to intolerable levels.

Our growth assay demonstrates that sustained TRPV1 activation produces similar long-term effects on survival of yeast and metazoan cells. Furthermore, activation of TRPV1 in yeast by thermal or chemical stimuli occurs on a physiologically relevant timescale, shown by visualizing TRPV1-mediated cobalt accumulation as a direct, short-term assay of channel activity. Stimulus-dependent uptake of cobalt chloride into TRPV1-expressing cells is observed following addition of ammonium sulfide, which generates a readily visible black cobalt sulfide precipitate (Winter, 1987; Wood et al., 1988). In TRPV1-expressing yeast, pellets from nonstimulated cells appeared off-white, but became deep black within 5 min of capsaicin treatment (Figure 1C), yielding a dose-response relationship consistent with previous functional assays (EC_{50} ~70 nM) (Figure 1D). As in the cell death assay, Kir2.1-transformed cultures did not respond to capsaicin, and capsaicin stimulation of TRPV1 in the absence of cobalt produced no color change. Similarly, TRPV1-expressing yeast responded robustly to a rise in bath temperature in a manner that closely parallels heat-evoked channel activation in electrophysiological studies (Figures 1C and 1E) (Caterina et al., 1997; Tominaga et al., 1998). Thus, our cobalt uptake assay illustrates that TRPV1 forms functional channels in yeast that are reminiscent of native or cloned channels expressed in vertebrate cells.

Unbiased Forward Genetic Screen Reveals Gain-of-Function Mutations

Constitutively active TRPV1 mutants might harbor deficits in some aspect of channel activation, and a comprehensive list of such mutations could provide valuable information about the location of the channel gate. We used the activity-dependent death phenotype described above to identify such TRPV1 alleles that, unlike the wild-type channel, conferred significant toxicity even under basal conditions (i.e., in the absence of capsaicin at 30°C). To execute this screen, we introduced a library of randomly mutagenized TRPV1 cDNAs into yeast and plated transformants onto medium containing ruthenium red, thereby blocking TRPV1 to allow for growth of all cells independent of channel activity. Resulting colonies were replica plated onto medium lacking ruthenium red to unmask the lethality of any constitutively active channels (Figure 2A). Colonies showing reduced survival in the absence of ruthenium red were picked from the original plate and retested to confirm their phenotype.

From this screen, we recovered TRPV1 alleles showing a range of toxic effects (Figure 2B). Out of approximately 46,000 clones examined, 46 reproducibly exhibited growth impairment in the absence of ruthenium red, yielding an overall hit rate of 0.1% (see Table S1 available online). This is in reasonable agreement with the hit rate obtained from a luminometry-based screen for gain-of-function alleles in the yeast TRP channel Yvc1p (Su et al., 2007; Zhou et al., 2007) and is consistent with the general principle that gain-of-function mutations in channels are rare.

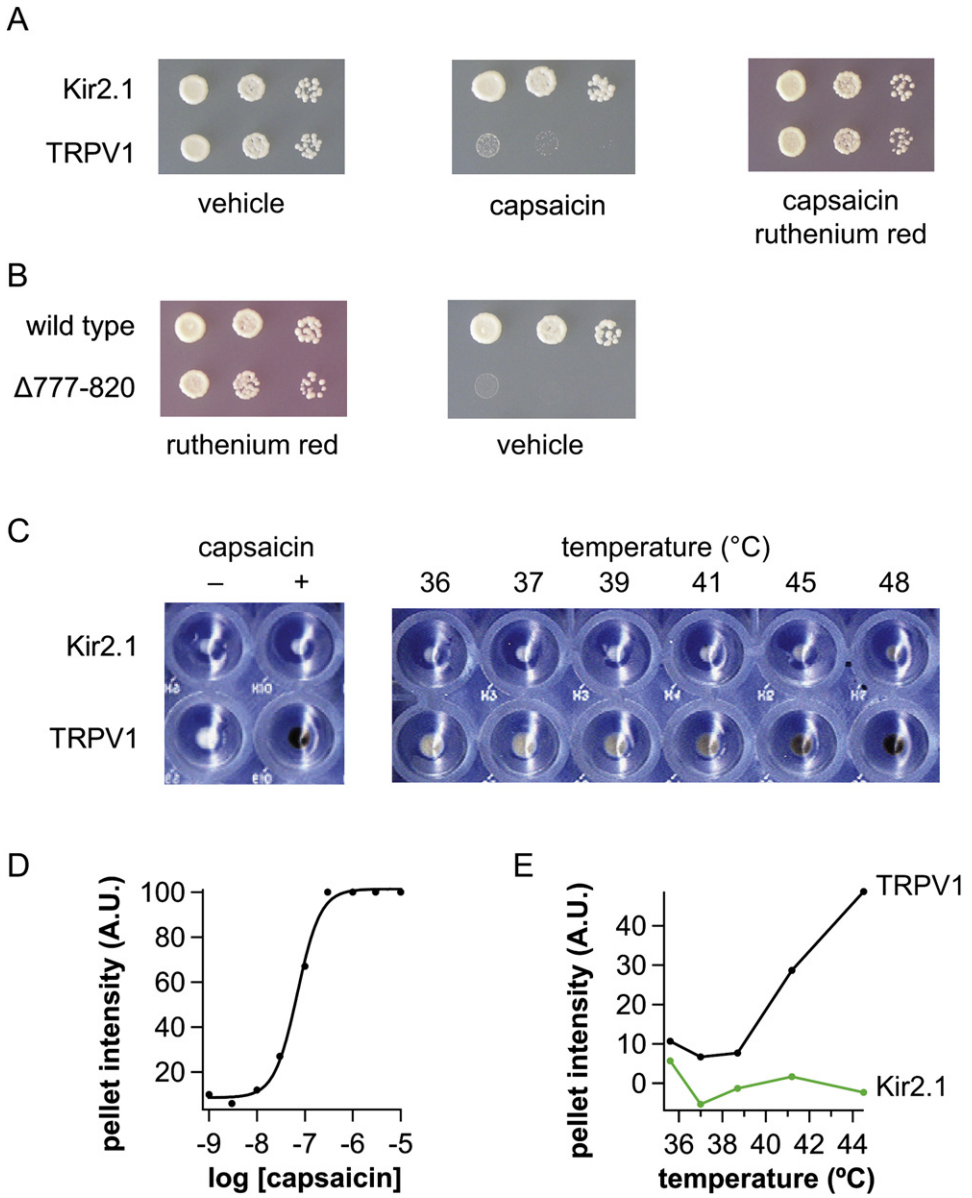

Figure 1. Mammalian TRPV1 Forms Functional Channels in Yeast

(A) Serial dilution assay for growth of yeast strains transformed with plasmids encoding mouse Kir2.1 or rat TRPV1. Yeast were resuspended to approximately the same density, spotted (from left to right) on indicated media and allowed to grow at 30°C for 3 days.

(B) Serial dilution assay for wild-type TRPV1 versus TRPV1 Δ777-820, grown as described in (A).

(C) Representative cobalt uptake assay performed with yeast expressing TRPV1 or Kir2.1. Cells were exposed to 10 μM capsaicin (at 30°C) or elevated bath temperature (36°C–48°C) and cobalt accumulation visualized in cell pellets collected in microtiter wells.

(D) Intensity of cobalt sulfide staining was determined using pixel quantitation (arbitrary units), yielding a capsaicin concentration response relationship that could be fit with a sigmoid function.

(E) Quantitation of TRPV1 (black) or Kir2.1 (green) temperature responsiveness in yeast using the cobalt uptake assay, revealing a TRPV1 thermal activation threshold near 40°C.

Our set of TRPV1 gain-of-function alleles defined a total of 30 unique mutations at 25 amino acid positions (Table S2). Interestingly, recovered mutations were clustered within the presumptive pore and cytoplasmic termini (Figure 2C). Only two gain-of-function mutations were recovered within the first four transmembrane domains, even though sequencing of randomly selected library clones showed equal mutagenic frequency throughout the coding region. Given the architectural similarity between TRP and voltage-gated channels and the critical role played by the first four transmembrane helices in voltage sensitivity, we were surprised to observe a relative paucity of gain-of-function alleles within this module.

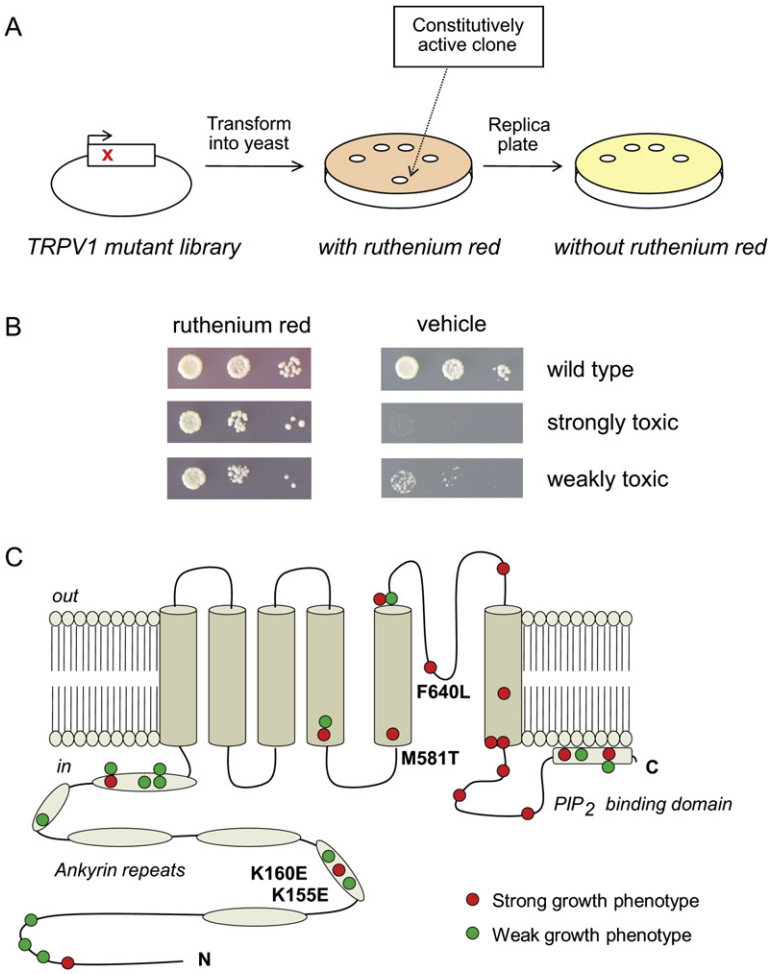

Figure 2. Yeast Genetic Screen Identifies Gain-of-Function TRPV1 Alleles

(A) Outline of the screening procedure: yeast were transformed with the randomly mutagenized TRPV1 library and grown for 2 days following replica plating. Subsequently, toxic alleles were identified and picked from the ruthenium red plate for secondary analysis and plasmid rescue.

(B) Serial dilution assays of cultures expressing wild-type TRPV1 or representative mutants, illustrating the range of toxic phenotypes recovered from the yeast screen.

(C) Each allele recovered in the screen was mapped onto a topology diagram of TRPV1. Red or green spheres indicate location of mutations causing strong or weak toxic phenotypes, respectively. N-terminal ankyrin repeats, transmembrane helices (S1–S6), and putative C-terminal PIP_2 binding domain are shown. Mutants exhibiting high constitutive activity in electrophysiological assays (see Figure 3) are labeled for reference.

Electrophysiological Analysis Reveals a Range of Functional Alterations

We used electrophysiological methods to directly characterize the functional properties of mutant channels when expressed in *Xenopus* oocytes. For all channels, basal and proton-evoked currents were assessed at pH 7.4 and 6.4, respectively, and normalized to a saturating concentration (10 μM) of capsaicin. As expected, wild-type TRPV1 responded strongly to capsaicin but displayed negligible current under basal conditions or in response to pH 6.4 (Figure 3A), which is just at the threshold concentration required for proton-evoked activation at room temperature (Chuang et al., 2001; Jordt and Julius, 2002; Tominaga et al., 1998). In contrast, eight of the recovered mutants displayed a significant response to pH 6.4, although no basal current was detected at pH 7.4 (Figures 3B and 3E). We labeled such mutants as "potentiated." Furthermore, a second group of mutants displayed a more extreme phenotype, manifest as large basal currents at pH 7.4 (≥15% of the maximum capsaicin-evoked response) (Figures 3C–3E). These basal currents showed characteristic outward rectification and block by ruthenium red, indicating that they are carried by TRPV1. We refer to these mutants as "constitutively active."

Among the constitutively active channels, residues K155 and K160 map to a single N-terminal ankyrin repeat domain, while M581T and F640L are in the S5-pore-S6 region (Figure 2C). Interestingly, the two N-terminal lysine residues have been previously shown to bind cytoplasmic ATP and calmodulin (Lishko et al., 2007). Lysine-to-alanine substitutions at these positions abolish interaction with ATP or calmodulin and reduce tachyphylaxis (the process by which repeated channel stimulation evokes progressively weaker responses), thereby decreasing efficiency of channel closure upon repeated stimulation. These mutants also display hypersensitivity to capsaicin (Lishko et al., 2007). We asked whether the glutamate substitutions identified by our screen are mechanistically equivalent to the previously described alanine substitutions. Indeed, both sets of substitutions led to comparable toxicity in yeast (Figure S1A) and high basal currents in oocytes (Figure S1B), presumably reflecting constitutive activity and/or a failure to desensitize. In any case, our independent identification of these mutations validates the ability of the yeast screen to pinpoint functionally significant TRPV1 residues.

In summary, three functionally distinct classes of TRPV1 alleles arose from our screen, ranging from mutations causing little perturbation of basal or stimulus-evoked activity to those causing dramatic constitutive activation. Interestingly, not all mutants arising from the screen exhibit marked electrophysiological phenotypes in oocytes. This disparity could reflect physiological differences between yeast and metazoan systems, such as transmembrane voltage (highly negative in yeast), growth temperature and extracellular pH, or differential expression of regulatory factors. Nonetheless, the screen has clearly enriched for mutants with heightened agonist sensitivity, consistent with our goal of identifying substitutions rendering TRPV1 constitutively active or hypersensitive.

F640L Renders Channels Hypersensitive to Thermal and Chemical Stimuli

Among the mutants displaying high constitutive activity in oocytes, we focused on F640L for three main reasons. First, F640L displayed the strongest basal channel activation of all

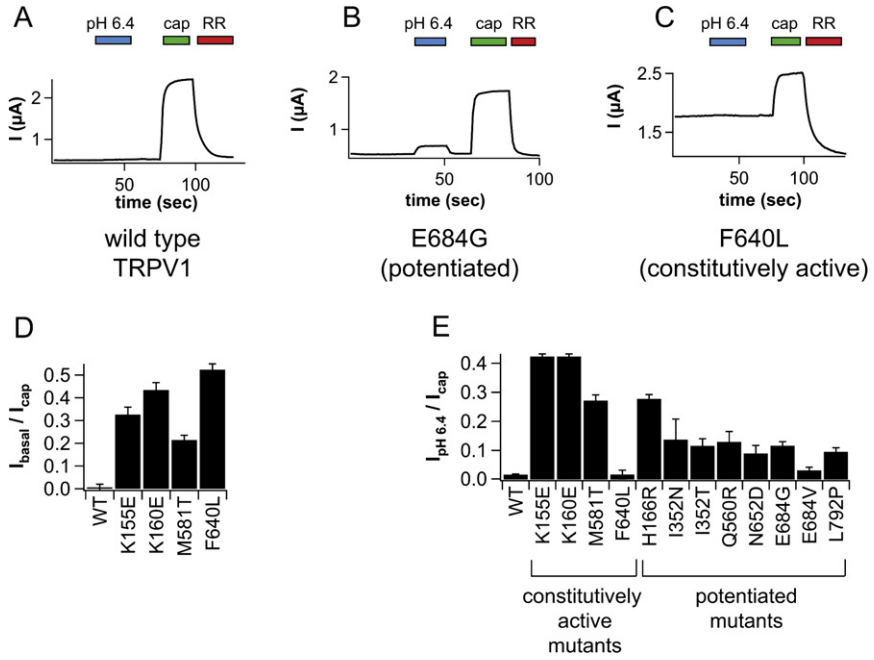

Figure 3. Mutants Recovered from the Yeast Screen Display Altered Electrophysiological Properties

Representative current traces from two-electrode voltage-clamp (TEVC, +80 mV) recordings of oocytes expressing wild-type TRPV1 (A), potentiated mutants (B), or constitutive mutants (C). Oocytes were challenged with protons (pH 6.4), capsaicin (10 μM), or ruthenium red (10 μM). (D) Quantitation of basal currents for all TRPV1 mutants exhibiting constitutive activity (normalized to a saturating capsaicin response; mean ± SEM, n ≥ 3 per construct). Currents in the presence of ruthenium red (10 μM) were used as baseline. For wild-type TRPV1, >90% block of capsaicin-evoked currents was achieved after 30 s of ruthenium red treatment, and the wild-type value of I_{basal}/I_{cap} was subtracted from all measurements. (E) Quantitation of pH 6.4 responses (normalized to a saturating capsaicin response) for all TRPV1 mutants exhibiting constitutive or potentiated activity. Data represent mean ± SEM, n ≥ 3 per construct.

mutants examined (Figures 3C and 3D), suggestive of a dramatic alteration in TRPV1 function. Second, F640 lies within the presumptive TRPV1 outer pore, a region that remains relatively unexplored with regard to TRP channel gating. Finally, the F640L allele displayed a unique phenotype in regard to basal versus proton-evoked currents, as described in more detail later.

We examined the biophysical properties of the F640L mutant by patch-clamp recording of transfected HEK293 cells. Consistent with its yeast phenotype, the F640L mutant conferred substantial toxicity when expressed in HEK293 cells, characterized by necrotic morphology similar to that observed in cells expressing wild-type TRPV1 after prolonged exposure to capsaicin (Caterina et al., 1997) (Figures 4A and 4B). Inclusion of ruthenium red (3 μM) in the culture medium significantly attenuated the death of F640L-expressing cells, permitting electrophysiological analysis.

We examined the sensitivity of F640L mutant channels to chemical and thermal stimuli. Inside-out membrane patches from HEK293 cells expressing wild-type TRPV1 showed small but measurable basal activity at room temperature that exhibited strong outward rectification (i.e., negligible inward current at −60 mV), consistent with previous reports (Chuang et al., 2001; Matta and Ahern, 2007). Subsequent challenge of these cells with a saturating dose of capsaicin (10 μM) elicited a large (~200-fold) induction of the basal current (Figure 4C). In contrast, inside-out patches from the F640L mutant routinely displayed large basal currents with a substantial inward component (Figure 4D). Despite this difference in basal activity, addition of capsaicin at saturating concentrations produced currents of similar magnitude to those evoked in patches containing wild-type channels. We found no significant difference in either the single-channel conductance or the relative permeabilities for Na^+, K^+, and Ca^{2+} ions when comparing wild-type and F640L mutant channels (Figure S2), showing that the F640L mutation affects gating rather than permeation properties.

Consistent with a hypersensitive gating mechanism, we found that the F640L mutant displayed a 35-fold leftward shift in the capsaicin dose-response curve compared to the wild-type receptor (EC_{50} = 1.91 ± 1.26 and 65.62 ± 4.03 nM, respectively) (Figure 5A). Interestingly, mutant channels also exhibited a lower Hill coefficient (0.33 ± 0.08 versus 2.06 ± 0.20 for wild-type TRPV1), indicative of decreased agonist cooperativity. Importantly, the basal F640L-mediated current was suppressed by the inverse agonist capsazepine (Figure 5D), demonstrating that the high constitutive activity is not due to an inability of the channel to close. This mutant also exhibited robust currents well below room temperature, corresponding to a dramatic shift in thermal activation threshold (Figure 5B) that resembles a proton-potentiated response in cells expressing wild-type TRPV1 (Jordt et al., 2000; Tominaga et al., 1998). Because the basal responsiveness of the F640L mutant was reduced with decreased ambient temperature, the mutant phenotype is unlikely to result from a defect in temperature detection per se, but rather from an independent mechanism that more generally affects gating. Our data suggest that the gating machinery remains intact in the F640L mutant, but the equilibrium has shifted to favor the open state.

F640L Mimics and Occludes Proton-Mediated Channel Potentiation

In contrast to all other mutants in the high constitutive activity group, only the F640L basal currents were not further potentiated under low pH conditions (Figure 3E). Nonetheless, addition of capsaicin to F640L-expressing cells led to a marked increase in current, demonstrating that F640L channels are not maximally open in the basal state (Figures 3C and 4D). As such, the failure to observe proton-evoked potentiation likely reflects a perturbation in the gating mechanism through which protons exert their physiological regulatory effect on TRPV1.

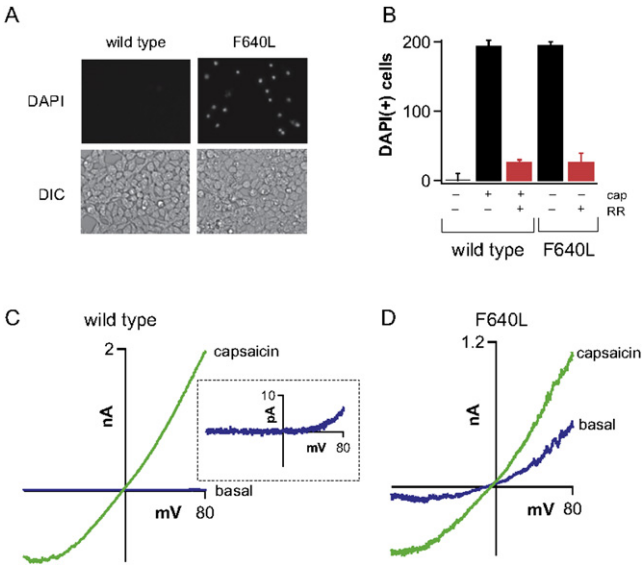

Figure 4. F640L Mutant TRPV1 Channels Are Toxic and Display High Basal Activity in Mammalian Cells

(A) Representative image of HEK293 cells transfected with wild-type TRPV1 or F640L mutant after staining with 4′,6-diamidino-2-phenylindole (DAPI) to identify dead cells. Corresponding differential interference contrast (DIC) images are shown below.

(B) Quantitation of cell death assay as performed in (A). Black and red bars represent cell death in the absence or presence of ruthenium red (3 μM, RR), respectively (mean ± SEM). Death among cells transfected with wild-type TRPV1 with or without capsaicin (1 μM, cap) is shown for comparison. Background cell death was determined from cells transfected with vector alone and subtracted from each measurement.

(C and D) Representative inside-out patch recording from HEK293 cells transfected with wild-type TRPV1 or the F640L mutant. Voltage ramps under basal conditions (blue) or in the presence of 10 μM capsaicin (green) are shown. (Inset) For the wild-type channel, 25 consecutive ramp traces were averaged and leak-subtracted to accurately derive the ensemble average basal current.

In mammalian cell patch-clamp experiments, we found that, although the wild-type channel was potentiated by exposure to pH 6.2, the F640L current was completely unaffected under these conditions (Figures 5C–5E), demonstrating a defect in proton-evoked potentiation. We also observed that a weakly alkaline solution (pH 8.2) failed to reduce the F640L-mediated basal current, even though the same conditions suppressed currents evoked by a moderate dose of capsaicin (70 nM) in cells expressing the wild-type channel (data not shown). However, higher doses of protons could activate the F640L mutant in a manner similar to the wild-type channel (pH_{50} = 5.60 ± 0.03 versus 5.72 ± 0.19 for wild-type and F640L mutant channels, respectively), illustrating that while the mutant has lost the ability to be potentiated within a certain pH range, its proton activation has not been completely ablated.

Taken together, our data show that the F640L mutation enhances sensitivity to heat and capsaicin by shifting the stimulus-response relationships of the channel leftward while also decreasing apparent cooperativity of gating. Indeed, this phenotype closely resembles that of wild-type TRPV1 channels operating under acidic conditions. In contrast, the sensitizing effects of extracellular protons are lost in the F640L channel, as one might expect if this mutation phenocopies the proton potentiated state.

Additional Substitutions in the Outer Pore Alter TRPV1 Gating

The F640 residue is located near the C-terminal end of a 15 amino acid stretch immediately preceding the presumptive selectivity filter, a region known in K^+ channels as the pore helix (Doyle et al., 1998). While TRP and K^+ channels share limited homology, computer algorithms (Jones, 1999) predict a high degree of helicity in this region of TRPV1, suggesting that a pore helix may indeed be present (Figure 6A). While it is generally accepted that the outer pore region contains structural determinants for ion permeation and block (Yellen, 1998), the role of pore helices in the regulation of channel gating has been less fully explored. Our yeast screen and functional characterization of F640L suggest that the pore helix may be particularly critical for TRPV1 gating.

We randomized the F640 codon to fully explore the structural requirements at this position (Figure 6B). Transformants from an F640 minilibrary were evaluated for wild-type, gain-of-function, or loss-of-function behavior using the yeast growth assay. Most substitutions at this position, particularly those of a hydrophilic nature, weakened or abolished channel activity. In contrast, several hydrophobic amino acids supported wild-type functionality, except for leucine and isoleucine, which produced constitutively active channels. Thus, our codon randomization illustrates that most hydrophobic substitutions at F640 produce functional channels, whereas two small hydrophobic residues support constitutive channel activity, suggesting that F640 is buried in a nonpolar environment.

Although we analyzed a large number of clones in our initial yeast screen, it is possible that some function-altering substitutions went undetected. We therefore screened a more restricted yeast library in which only the TRPV1 pore helix and its immediate environment (residues 626–660) were randomly mutagenized to uncover additional substitutions in this region that might lead to constitutive activation (Table S1). We uncovered nine additional substitutions conferring a toxic phenotype in yeast. Of these, two (N628D and V658A) showed a potentiation effect under moderately acidic conditions, while two more (T641S and T650S) showed high basal activity (Figures 6C and 6D). Interestingly, T641S (and, to a lesser extent, T650S) mutants displayed large constitutive channel activation with relative insensitivity to pH 6.4. The T641S mutant also caused widespread death in HEK293 cells (data not shown). Thus, at least two mutants recovered in the outer pore region are reminiscent of the original F640L mutation. Because substitutions in two adjacent residues (F640 and T641) produce similar functional alterations, we conclude that the short stretch of amino acids at the interface between the pore helix and the permeation pathway forms a particularly crucial part of the gating apparatus.

The Functional Role of the Pore Helix Is Conserved in Related TRP Family Members

Mammalian TRPV channels are highly divergent at the amino acid level. Rat TRPV1, TRPV2, TRPV3, and TRPV4 exhibit only 21% identity overall, while TRPV5 and TRPV6 are even more distantly related. Interestingly, the 13 residue long stretch

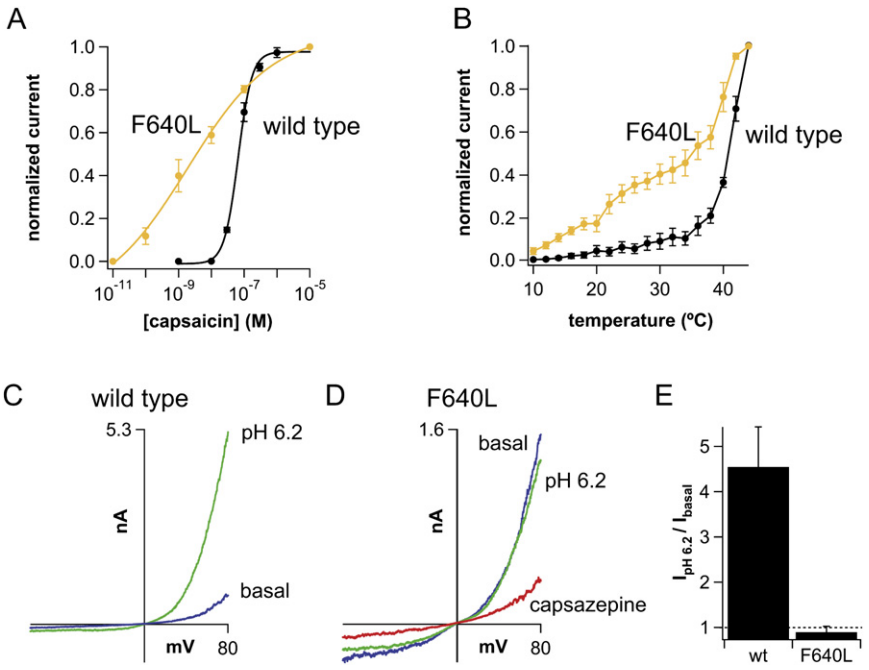

Figure 5. F640L TRPV1 Mutant Channels Show Enhanced Chemical and Thermal Sensitivity, but Decreased Proton Potentiation

(A) TEVC recording of TRPV1 wild-type (black) or F640L (orange) channels reveals leftward shift in the agonist dose-response relationship (mean ± SEM at +80 mV, n = 4 oocytes per condition).

(B) Inside-out patch recording from HEK293 cells transfected with wild-type (black) or F640L (orange) channels stimulated with a temperature ramp from 10°C to 44°C (mean ± SEM at −60 mV, n ≥ 4 patches per condition) reveals hypersensitivity to heat.

(C and D) Voltage-ramp traces from whole-cell patch-clamp recordings of HEK293 cells expressing wild-type or F640L mutant channels. Blue traces indicate basal channel current at room temperature in pH 7.4 bath solution, while green traces indicate channel current after perfusion with pH 6.2 bath solution. Subsequent addition of capsazepine (30 μM, red) efficiently inhibited F640L basal current.

(E) Quantitation of fold potentiation (at +80 mV) at pH 6.2 versus 7.4 for wild-type and F640L channels, as in (C) and (D) (mean ± SEM, n = 4–6 cells per condition).

connecting the pore helix and selectivity filter displays 69.2% identity in TRPV1–4 (Figure 6A), suggesting that some TRP channels may share common architectural features within this region. We therefore asked whether any pore helix mutations identified in our TRPV1 screen would produce a gain-of-function effect in other TRPV family members.

TRPV3 is activated by warm temperatures, with a threshold in the 33°C–38°C range (Peier et al., 2002; Smith et al., 2002; Xu et al., 2002). Sequence alignments reveal a threonine at position 636 in TRPV3 corresponding to T641 in TRPV1 (Figure 6A). We asked whether TRPV3 T636S channels displayed constitutive activity similar to TRPV1 T641S. Strikingly, transfection of TRPV3 T636S into HEK293 cells produced massive cell death that was significantly attenuated by ruthenium red, while no toxicity was observed from the wild-type channel (Figure 7D). In inside-out patches excised from oocytes expressing wild-type TRPV3, we observed small outwardly rectifying basal currents that were robustly stimulated by the broad-spectrum TRP channel agonist 2-aminoethoxydiphenyl borate (2-APB) (Chung et al., 2004a; Hu et al., 2004) (Figure 7A). In contrast, TRPV3 T636S exhibited large basal currents characterized by high channel noise and outward rectification (Figure 7B), reminiscent of wild-type TRPV3 activity at warm temperatures. As with the TRPV1 pore helix mutant, TRPV3 T636S channels showed substantial basal currents at negative holding potentials. By normalizing the basal currents to a maximal 2-APB-evoked response (300 μM), we estimate that T636S displays ~300-fold increase in spontaneous activity compared to the wild-type channel (Figure 7C). TRPV3 T636S basal currents were suppressed by cold (10°C), and the inward current was strongly attenuated by ruthenium red (Figures 7A and 7B and

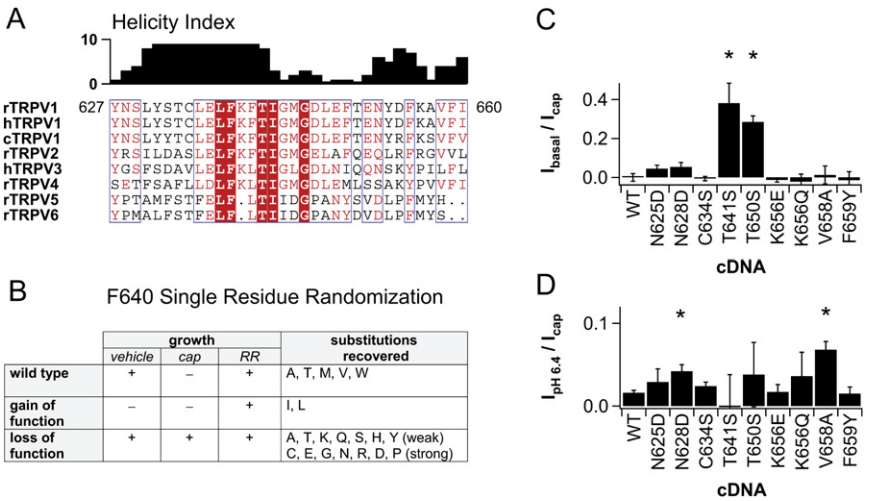

Figure 6. Additional Substitutions in the TRPV1 Pore Helix Affect Channel Activation

(A) Alignment of the pore helices and selectivity filters from various TRPV channels (r, rat; h, human; c, chicken). Helicity index for rat TRPV1 (0–10, generated using PSIPRED) is shown above alignment.

(B) Summary of F640 saturation screen. Transformants harboring a library of TRPV1 mutants (with a randomized F640 codon) were scored according to growth pattern and mutant plasmids sequenced to determine the amino acid substitution. Note that F640A and F640T were scored as both "wild-type" and "weak loss of function," consistent with an intermediate phenotype.

(C and D) Quantitation of normalized basal or pH-evoked currents for mutants recovered from the pore helix screen, analyzed by TEVC as in Figure 3. *p ≤ 0.01, Student's t test.

Data represent mean ± SEM, n ≥ 3 per construct.

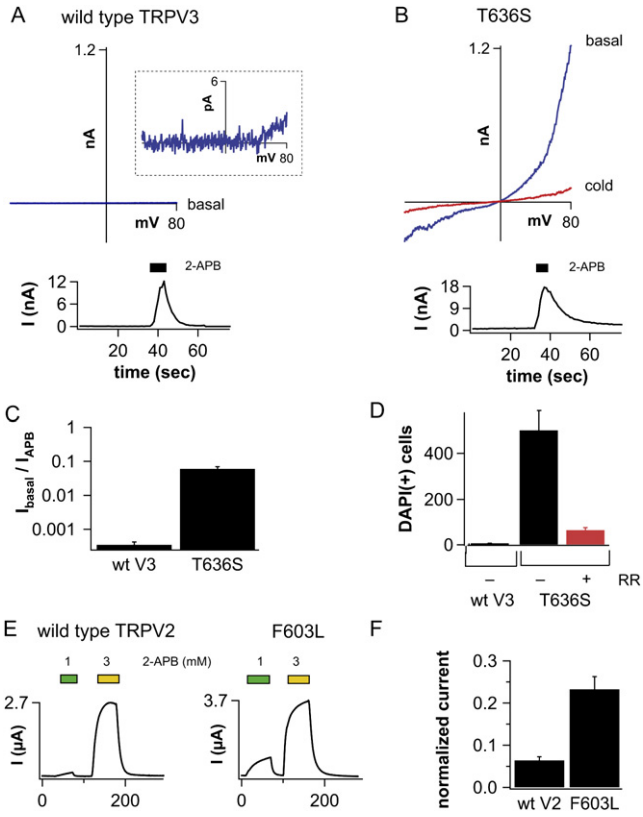

Figure 7. The Gating Function of the Pore Helix Is Conserved across TRPV Channels

Voltage-ramp traces from representative inside-out macropatches excised from oocytes expressing wild-type human TRPV3 (A) versus T636S mutant (B). Patches were allowed to stabilize for 5 min after excision. Blue traces indicate basal current at room temperature. Inset represents ensemble average basal current for wild-type TRPV3. Red trace shows current at 10°C, illustrating block of T636S basal activity by cold temperature. Corresponding current versus time plots are shown below each set of voltage ramps, illustrating that wild-type and mutant channels respond similarly to 300 μM 2-APB. (C) Quantitation of basal current (normalized to 300 μM 2-APB response) for TRPV3 wild-type or T636S mutant channels ($n \geq 4$ patches per condition). (D) TRPV3 T636S mutant caused massive toxicity in transfected HEK293 cells that was blocked by ruthenium red (RR, 3 μM, red bar). Wild-type TRPV3 is shown for comparison (mean ± SEM). (E) Representative traces from TEVC recordings of oocytes expressing wild-type rat TRPV2 versus F603L mutant. Oocytes were exposed to 1 or 3 mM 2-APB (green or yellow bars, respectively). (F) Quantitation of 1 mM 2-APB evoked responses in cells expressing wild-type TRPV2 or F603L mutant channel (normalized to the 3 mM 2-APB response) reveals that the F603L mutant displays enhanced sensitivity to a lower concentration of 2-APB (mean ± SEM; n = 4 cells per condition; $p \leq 0.001$, Student's t test).

data not shown), a pharmacology consistent with TRPV3-evoked currents in native or heterologous systems (Chung et al., 2004b; Peier et al., 2002; Smith et al., 2002; Xu et al., 2002). We also investigated the effects of an F603L substitution in TRPV2, a position corresponding to F640L in TRPV1. Unlike other TRPV channels, wild-type TRPV2 exhibits no measurable basal activity when heterologously expressed, and we did not detect basal currents from either wild-type or F603L TRPV2 channels (data not shown). Nevertheless, we observed that the F603L mutant displays enhanced 2-APB sensitivity (Figures 7E and 7F). Taken together, our data show that mutations in pore helices shift multiple TRPV channels into an open conformation, showing that this region plays a conserved role in the gating of different TRP family members by diverse chemical and thermal stimuli.

DISCUSSION

Conservation of TRPV1 Functional Properties in a Nonmammalian Genetic System

Spontaneous gain-of-function mutations have provided valuable insights into ion channel permeation and gating (Kohda et al., 2000; Navarro et al., 1996). While naturally occurring mutations have been identified in mammalian TRP channels (Asakawa et al., 2006; Kim et al., 2007; Xu et al., 2007), these sporadic genetic events are too rare to support a systematic analysis of TRP channel functionality. Here, we report a facile and unbiased forward genetic screen for isolating gain-of-function mutations in a mammalian TRP channel based on a simple yeast growth phenotype. This high-throughput methodology enabled us to survey the TRPV1 coding region for substitutions that cause constitutive activation. Such an approach has been applied to microbial cation channels (Loukin et al., 1997; Ou et al., 1998) and vertebrate inward rectifier K^+ channels (Sadja et al., 2001; Yi et al., 2001), and we now extend this strategy to include nonselective mammalian cation channels. Previous studies have exploited polymorphisms between TRP channel homologs or orthologs to delineate molecular determinants underlying ligand activation (Chuang et al., 2004; Jordt and Julius, 2002; Ryu et al., 2007), but this methodology is limited for numerous reasons. TRP channel subtypes generally exhibit low sequence homology, and thus channel chimeras are often nonfunctional. In addition, such an approach cannot pinpoint residues that are conserved across channels. Indeed, many mutations uncovered by our screen are highly conserved in TRPV1 orthologs or other TRPV family members, attesting to the increased power of this approach for detecting core structural elements. A select percentage (0.10%) of mutant channels emerged from the cell death assay, of which ~40% showed bona fide functional perturbations when examined in vertebrate expression systems, attesting to both the stringency and efficiency of the screen. Perhaps most importantly, this screen revealed a number of interesting channel mutants that have not been described in previous structure-function studies.

Remarkably, rat TRPV1 expressed in yeast recapitulates functional properties observed in neurons or other mammalian cell types, including sensitivity to noxious heat and capsaicin. This suggests that both chemical and thermal sensitivity are intrinsic channel properties, not requiring membrane or cytoplasmic factors specific to metazoans. Moreover, yeast are hyperpolarized compared to metazoan cells, with membrane potentials estimated at −100 to −250 mV (Serrano and Rodriguez-Navarro, 2001). The observation that TRPV1 can be robustly activated in yeast therefore favors a modest role for membrane voltage as a regulator of channel gating (Latorre et al., 2007; Matta and Ahern, 2007).

The Pore Helix as a Transducer of TRPV1 Gating

A hallmark of many TRP channels is their ability to integrate multiple physiological inputs (Clapham, 2003; Dhaka et al., 2006; Julius, 2005). This is exemplified by TRPV1, whose role as a polymodal detector of chemical and physical stimuli underlies its capacity to regulate sensory neuron excitability under normal and pathophysiological conditions (Tominaga et al., 1998). Different TRPV1 stimuli (e.g., capsaicin, heat, acidic pH) produce synergistic effects on channel activation, while antagonists (e.g., capsazepine, cold, alkaline pH) diminish responses to multiple activating stimuli, providing evidence for crosstalk and convergence in channel gating mechanisms (Tominaga et al., 1998). This is consistent with our observation that the F640L mutant shows a shallowing of dose-response profiles to capsaicin and temperature, accompanied by a leftward shift in activation thresholds. This decreased cooperativity and increased sensitivity suggest that the pore helix region undergoes a structural transition common to all activating modalities, for which the energetic barrier is lowered by mutations such as F640L.

In the case of extracellular protons, it is possible to separate their ability to potentiate other stimuli under moderately acidic (pH 6.4) conditions versus their ability to activate TRPV1 de novo at room temperature (pH < 6.0). Mutations at two extracellular glutamate residues, E600 or E648, selectively alter the modulatory versus activating effects of protons, respectively (Jordt et al., 2000). In this regard, it is interesting that F640L displays agonist hypersensitivity and loss of proton-mediated potentiation but shows normal de novo gating by protons, similar to positively charged substitutions at E600 (Jordt et al., 2000). Thus, perturbations in the pore helix are sufficient to favor an open conformation, perhaps mimicking and occluding the modulatory effect mediated by interaction of protons with extracellular sites such as E600.

While our data establish a role for the pore helix in proton-mediated potentiation, recent work suggests that this domain may also be involved in de novo proton gating. Mutation of residue T633 in TRPV1, also located within the pore helix, abolishes proton-evoked activation, although protons can still potentiate currents evoked by capsaicin (Ryu et al., 2007). Thus, other pore helix substitutions show a distinct but related phenotype to that observed in our study, namely, alteration of de novo proton-evoked activation rather than proton-mediated potentiation. These studies support the general conclusion that conformational changes in the pore helix are critical for both the activating and modulatory effects of protons on TRPV1 and underscore the idea that, while proton-mediated potentiation and de novo activation are determined by distinct sets of residues, their effects on channel gating both involve the pore helix as a key regulatory domain.

Based on secondary structure predictions and their relationship to known K^+ channel structures, E600 and E648 are predicted to lie near the extracellular face of the outer pore, close to the top of the pore helix (Figure 8), and it is conceivable that protonation of these residues could induce conformational rearrangements propagating through the pore helix that ultimately lead to channel opening. Perhaps the C terminus of the pore helix forms a movable barrier to ion flux, either by protruding directly into the permeation pathway or by constricting the selectivity filter into a nonconductive conformation similar to that observed in one crystal structure of the prokaryotic K^+ channel KcsA (Zhou et al., 2001). Alternatively, residues within the pore helix might not form a physical occlusion per se, but rather stabilize an open conformation of the channel, comparable to a model proposed for the gating of inward rectifier K^+ channels (Alagem et al., 2003).

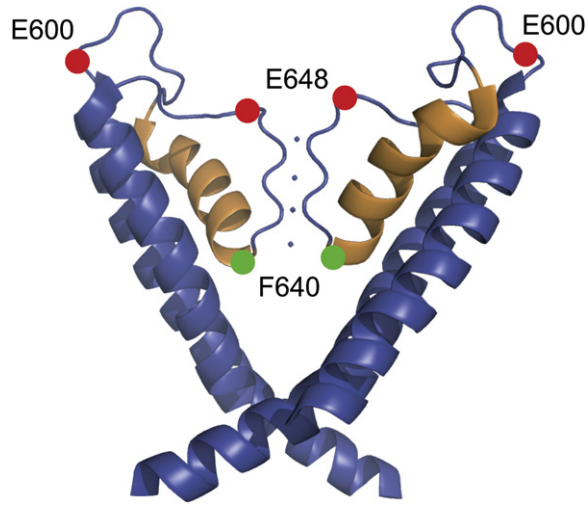

Figure 8. A Structural Model for the Pore Region of TRP Channels
A model of the S5-pore-S6 region of TRPV1 as inspired by the Kv1.2 structure (PDB: 2R9R), prepared with PyMOL software (Delano, 2002). The pore helix is shown in orange. Relative location of the F640 residue is shown in green, and E600 and E648 residues previously implicated in proton modulation are shown in red.

The Pore Helix as a Conserved Element in TRP Channel Gating

Our present analysis of the pore helix suggests that its role in gating is conserved in at least a subset of TRP channels. We found that mutation of pore helix residues leads to constitutive activation of TRPV3, as well as potentiation of TRPV2. Therefore, our study suggests that the pore helix plays a general role in TRP channel gating that has not been previously appreciated. TRPV1 may represent a case in which a universal gating element has been usurped to serve as an allosteric regulatory site for protons, allowing for alteration of TRPV1 sensitivity in the setting of inflammation and tissue acidosis. Thus far, relatively few structural elements have been shown to play conserved functional roles in TRP channels, and it may be worthwhile to investigate pore helices as gating elements in other mammalian TRP family members.

While numerous studies have localized the molecular determinants of ion permeation and block to the outer pore region of TRP (Voets et al., 2002, 2004) and other cation channels (Ahern et al., 2006; Chatelain et al., 2005; Doyle et al., 1998), the role of the pore helix in TRP channel gating and agonist sensitivity is unexpected. Indeed, structural analyses suggest that voltage activation of K^+ channels involves alteration of interactions between the S4-S5 linker and the cytoplasmic end of S6, relieving strain on the helical bundle crossing that forms the intracellular gate (Long et al., 2005a, 2005b; Tombola et al., 2006). In this model, the outer pore region is an ion conduit that remains relatively stationary during the overall gating transition. On the other hand, the

outer pore is known to play a critical role in the context of C-type inactivation, the process by which repetitive voltage stimulation desensitizes voltage-gated K^+ channels via a mechanism involving collapse of the selectivity filter. Mutations in the outer pore region, including the pore helix, can dramatically influence the extent of K^+ channel C-type inactivation, suggesting that these regions play an important role in modulating the biophysical properties of open K^+ channels (Cordero-Morales et al., 2006; Hoshi et al., 1991; Liu et al., 1996; Lopez-Barneo et al., 1993). Thus, the outer pore can influence the level of K^+ channel activity under certain conditions.

Aside from K^+ channels, additional studies have suggested a role for the pore helix in gating of other 6TM channels. Cysteine accessibility experiments in CNG channels (Liu and Siegelbaum, 2000), as well as in TRPV5 and TRPV6 (Voets et al., 2004; Yeh et al., 2005), show that residues in the pore helix are differentially reactive to modifying agents in the closed and open states, illustrating that in these cases (and unlike K^+ channels), the pore helix may rotate during gating. Together with our findings, these observations indicate that, despite topological resemblance to voltage-gated K^+ channels, gating of other members of the 6TM superfamily may involve a conformational change in the outer pore region. This is not to say that the structural determinants of activation identified in voltage-gated channels are irrelevant to TRP channels. Indeed, recent work has identified spontaneous dominant mutations in TRPV3 linked to hair loss and atopic dermatitis that dramatically enhance basal activity when engineered into the cloned channel (Asakawa et al., 2006; Xiao et al., 2007). Interestingly, both mutations map to a single residue in the putative S4-S5 region of TRPV3, suggesting that conformational changes in this linker might also play a role as molecular determinants of channel activation, perhaps via interaction with a cytoplasmic activation gate at the intracellular segment of S6. These and other studies highlight the idea that TRP channel gating likely involves multiple regions, including the pore helix and the S4-S5 linker. Future work will address the physical and functional interplay between these regions in shaping the physiological properties of TRP channels.

EXPERIMENTAL PROCEDURES

Molecular Biology

Rat TRPV1 was cloned into p425GPD. For mutagenic library construction, TRPV1 was amplified using *Taq* polymerase (New England Biolabs) under standard conditions for 25 cycles, and the mutagenized N- or C-terminal cassettes were separately reintroduced back into the wild-type construct to generate two distinct libraries with the desired mutagenesis frequency. For the pore helix library, mutagenesis rate was boosted by supplementing the PCR with $MgCl_2$ and $MnCl_2$ (final concentrations of 7 and 0.5 mM, respectively), increasing cycle number to 40, and decreasing the concentration of dATP and dGTP relative to dCTP and dTTP. Site-directed mutagenesis was performed by overlap extension PCR or QuikChange (Stratagene) or by yeast in vivo recombination. Mutant channels were cloned into the mammalian/oocyte expression vector pMO (gift of Lily Jan) for functional analysis. All constructs were verified by DNA sequencing.

Yeast Transformation and Replica Plating

Strain BY4741 (*Mat***a** *his3Δ1 leu2Δ0 met15Δ0 ura3Δ0*) was transformed with lithium acetate/polyethylene glycol and selected on medium lacking leucine. Media was supplemented with 20 mM MES and buffered to pH 6.2, under which conditions little or no inward current is observed in mammalian cells expressing TRPV1 (Figure 5C). Capsaicin (Tocris) and/or ruthenium red (Sigma) were added to molten agar prior to pouring. After 2 days growth on selective medium with 3 μM ruthenium red (mother plate), transformants were replica plated onto two plates, one lacking and another containing 10 μM ruthenium red (daughter plates), the latter designed to eliminate false positives arising from inefficient colony transfer from the mother plate. After two more days, the daughter plates were aligned to identify clones exhibiting basal toxicity. Clones from this first round of screening were retested by serial dilution. Plasmids were subsequently rescued and retransformed into fresh BY4741 to confirm the phenotype.

Cobalt Uptake Assay

Yeast cultures were grown to mid-log phase in selective medium and washed once in cobalt uptake assay buffer (in mM: 58 NaCl, 5 KCl, 2 $MgCl_2$-$6H_20$, 0.75 $CaCl_2$, 12 glucose, 137 sucrose, 10 HEPES, pH 7.4). Pellets were resuspended in assay buffer with 5 mM $CoCl_2$ plus varying concentrations of capsaicin and incubated for 5 min at 30°C. For temperature experiments, cells were subjected to varying temperatures for 5 min using a gradient PCR thermocycler (MJ Research). Cells were washed twice in assay buffer and stained with 1% $(NH_4)_2S$.

Mammalian Cell Culture and Electrophysiology

HEK293T cells were cultured and transfected as previously described (Chuang et al., 2004.) For some experiments, we generated stable tetracycline-inducible Flp-in T-rex HEK293 cell lines (Invitrogen) expressing wild-type TRPV1 or the F640L mutant. For whole-cell or excised patch recordings, bath solution contained (in mM) 140 NaCl, 10 HEPES, 1 $MgCl_2$-$6H_2O$, 1 EGTA, pH 7.4. Pipette solution was identical, except that CsCl was substituted for NaCl. For proton experiments, we substituted MES for HEPES in the bath and adjusted pH accordingly. For single-channel analysis, pipette solution contained 1 μM capsaicin. Relative permeabilities were estimated from reversal potential shifts between solutions containing (in mM) 10 HEPES, 10 glucose, and either 140 NaCl, 140 KCl, or 125 NMDG-Cl + 10 $CaCl_2$. Liquid junction potentials did not exceed 3 mV. Pipettes were fabricated from borosilicate glass (WPI) with resistances after fire-polishing of 1–2 MΩ for whole-cell experiments, 0.8–1.2 MΩ for inside-out macropatch experiments, and 6–10 MΩ for cell-attached single-channel experiments. Currents were recorded with an Axopatch 200B amplifier (Molecular Devices) using a 180 ms voltage ramp from −120 mV to +80 mV delivered once per second. Currents were recorded at 5 kHz, filtered at 2 kHz, and analyzed with pClamp 10 (Molecular Devices). Temperature ramps were generated with a custom-made Peltier device (Reid-Dan Electronics). Capsaicin, capsazepine, and 2-APB were dissolved in DMSO, and ruthenium red was dissolved in water. Drugs were diluted into recording solution immediately prior to experiments.

Xenopus Oocyte Culture and Electrophysiology

Surgically extracted oocytes from *Xenopus laevis* (Nasco) were cultured and analyzed 2–14 days postinjection by TEVC as previously described (Chuang et al., 2004). For proton experiments, MES was substituted for HEPES and pH adjusted accordingly. For patch-clamp analysis, both the bath and pipette solutions contained (in mM) 140 CsCl, 10 HEPES, 1 $MgCl_2$-$6H_20$, 1 EGTA, pH 7.4. Macropatches were excised from devitellinized oocytes using pipettes with resistances of 0.3–0.8 MΩ, and currents were analyzed as described for mammalian cell patch clamp.

Mammalian Cell Death Assays

After 16 hr, transfected HEK293 cells were stained with DAPI (500 ng/ml) to identify dead cell nuclei. DAPI-positive cells were averaged from four different fields per transfection. Each field contained approximately the same total number of cells.

SUPPLEMENTAL DATA

The Supplemental Data for this article can be found online at http://www.neuron.org/cgi/content/full/58/3/362/DC1/.

ACKNOWLEDGMENTS

We thank members of the Julius lab for advice and encouragement at all stages of this project. We are especially grateful to D. Minor for valuable suggestions on establishing the yeast assays and H-h. Chuang, A. Priel, and Y. Kirichok for guidance on electrophysiological experiments. We thank H. Madhani, J. Weissman, and members of their labs for strains, plasmids, and assistance with yeast methods. We also thank R. Nicoll, D. Bautista, A. Chesler, D. Minor, and H-h. Chuang for insightful discussions and criticism of the manuscript. This work was supported by an American Heart Association Predoctoral Fellowship (B.R.M.), a UCSF Neuroscience NIH Training Grant (C.J.B.), and grants from the National Institutes of Health (NINDS) (D.J.).

Received: February 6, 2008
Revised: March 13, 2008
Accepted: April 11, 2008
Published: May 7, 2008

REFERENCES

Ahern, C.A., Eastwood, A.L., Lester, H.A., Dougherty, D.A., and Horn, R. (2006). A cation-pi interaction between extracellular TEA and an aromatic residue in potassium channels. J. Gen. Physiol. *128*, 649–657.

Alagem, N., Yesylevskyy, S., and Reuveny, E. (2003). The pore helix is involved in stabilizing the open state of inwardly rectifying K+ channels. Biophys. J. *85*, 300–312.

Asakawa, M., Yoshioka, T., Matsutani, T., Hikita, I., Suzuki, M., Oshima, I., Tsukahara, K., Arimura, A., Horikawa, T., Hirasawa, T., and Sakata, T. (2006). Association of a mutation in TRPV3 with defective hair growth in rodents. J. Invest. Dermatol. *126*, 2664–2672.

Bandell, M., Dubin, A.E., Petrus, M.J., Orth, A., Mathur, J., Hwang, S.W., and Patapoutian, A. (2006). High-throughput random mutagenesis screen reveals TRPM8 residues specifically required for activation by menthol. Nat. Neurosci. *9*, 493–500.

Caterina, M.J., Schumacher, M.A., Tominaga, M., Rosen, T.A., Levine, J.D., and Julius, D. (1997). The capsaicin receptor: a heat-activated ion channel in the pain pathway. Nature *389*, 816–824.

Chatelain, F.C., Alagem, N., Xu, Q., Pancaroglu, R., Reuveny, E., and Minor, D.L., Jr. (2005). The pore helix dipole has a minor role in inward rectifier channel function. Neuron *47*, 833–843.

Chuang, H.H., Prescott, E.D., Kong, H., Shields, S., Jordt, S.E., Basbaum, A.I., Chao, M.V., and Julius, D. (2001). Bradykinin and nerve growth factor release the capsaicin receptor from PtdIns(4,5)P2-mediated inhibition. Nature *411*, 957–962.

Chuang, H.H., Neuhausser, W.M., and Julius, D. (2004). The super-cooling agent icilin reveals a mechanism of coincidence detection by a temperature-sensitive TRP channel. Neuron *43*, 859–869.

Chung, M.K., Lee, H., Mizuno, A., Suzuki, M., and Caterina, M.J. (2004a). 2-aminoethoxydiphenyl borate activates and sensitizes the heat-gated ion channel TRPV3. J. Neurosci. *24*, 5177–5182.

Chung, M.K., Lee, H., Mizuno, A., Suzuki, M., and Caterina, M.J. (2004b). TRPV3 and TRPV4 mediate warmth-evoked currents in primary mouse keratinocytes. J. Biol. Chem. *279*, 21569–21575.

Clapham, D.E. (2003). TRP channels as cellular sensors. Nature *426*, 517–524.

Cordero-Morales, J.F., Cuello, L.G., Zhao, Y., Jogini, V., Cortes, D.M., Roux, B., and Perozo, E. (2006). Molecular determinants of gating at the potassium-channel selectivity filter. Nat. Struct. Mol. Biol. *13*, 311–318.

Decaillot, F.M., Befort, K., Filliol, D., Yue, S., Walker, P., and Kieffer, B.L. (2003). Opioid receptor random mutagenesis reveals a mechanism for G protein-coupled receptor activation. Nat. Struct. Biol. *10*, 629–636.

Delano, W.D. (2002). The PyMOL Molecular Graphics System (San Carlos, CA: DeLano Scientific).

Dhaka, A., Viswanath, V., and Patapoutian, A. (2006). Trp ion channels and temperature sensation. Annu. Rev. Neurosci. *29*, 135–161.

Doyle, D.A., Morais Cabral, J., Pfuetzner, R.A., Kuo, A., Gulbis, J.M., Cohen, S.L., Chait, B.T., and MacKinnon, R. (1998). The structure of the potassium channel: molecular basis of K+ conduction and selectivity. Science *280*, 69–77.

Gunthorpe, M.J., Harries, M.H., Prinjha, R.K., Davis, J.B., and Randall, A. (2000). Voltage- and time-dependent properties of the recombinant rat vanilloid receptor (rVR1). J. Physiol. *525*, 747–759.

Hoshi, T., Zagotta, W.N., and Aldrich, R.W. (1991). Two types of inactivation in Shaker K+ channels: effects of alterations in the carboxy-terminal region. Neuron *7*, 547–556.

Hu, H.Z., Gu, Q., Wang, C., Colton, C.K., Tang, J., Kinoshita-Kawada, M., Lee, L.Y., Wood, J.D., and Zhu, M.X. (2004). 2-aminoethoxydiphenyl borate is a common activator of TRPV1, TRPV2, and TRPV3. J. Biol. Chem. *279*, 35741–35748.

Jancso, G., Kiraly, E., and Jancso-Gabor, A. (1977). Pharmacologically induced selective degeneration of chemosensitive primary sensory neurones. Nature *270*, 741–743.

Jerman, J.C., Brough, S.J., Prinjha, R., Harries, M.H., Davis, J.B., and Smart, D. (2000). Characterization using FLIPR of rat vanilloid receptor (rVR1) pharmacology. Br. J. Pharmacol. *130*, 916–922.

Jones, D.T. (1999). Protein secondary structure prediction based on position-specific scoring matrices. J. Mol. Biol. *292*, 195–202.

Jordt, S.E., and Julius, D. (2002). Molecular basis for species-specific sensitivity to "hot" chili peppers. Cell *108*, 421–430.

Jordt, S.E., Tominaga, M., and Julius, D. (2000). Acid potentiation of the capsaicin receptor determined by a key extracellular site. Proc. Natl. Acad. Sci. USA *97*, 8134–8139.

Jordt, S.E., McKemy, D.D., and Julius, D. (2003). Lessons from peppers and peppermint: the molecular logic of thermosensation. Curr. Opin. Neurobiol. *13*, 487–492.

Julius, D. (2005). From peppers to peppermints: natural products as probes of the pain pathway. Harvey Lect. *101*, 89–115.

Jung, J., Lee, S.Y., Hwang, S.W., Cho, H., Shin, J., Kang, Y.S., Kim, S., and Oh, U. (2002). Agonist recognition sites in the cytosolic tails of vanilloid receptor 1. J. Biol. Chem. *277*, 44448–44454.

Kim, H.J., Li, Q., Tjon-Kon-Sang, S., So, I., Kiselyov, K., and Muallem, S. (2007). Gain-of-function mutation in TRPML3 causes the mouse varitint-waddler phenotype. J. Biol. Chem. *282*, 36138–36142.

Kohda, K., Wang, Y., and Yuzaki, M. (2000). Mutation of a glutamate receptor motif reveals its role in gating and delta2 receptor channel properties. Nat. Neurosci. *3*, 315–322.

Latorre, R., Brauchi, S., Orta, G., Zaelzer, C., and Vargas, G. (2007). ThermoTRP channels as modular proteins with allosteric gating. Cell Calcium *42*, 427–438.

Lishko, P.V., Procko, E., Jin, X., Phelps, C.B., and Gaudet, R. (2007). The ankyrin repeats of TRPV1 bind multiple ligands and modulate channel sensitivity. Neuron *54*, 905–918.

Liu, J., and Siegelbaum, S.A. (2000). Change of pore helix conformational state upon opening of cyclic nucleotide-gated channels. Neuron *28*, 899–909.

Liu, Y., Jurman, M.E., and Yellen, G. (1996). Dynamic rearrangement of the outer mouth of a K+ channel during gating. Neuron *16*, 859–867.

Long, S.B., Campbell, E.B., and Mackinnon, R. (2005a). Crystal structure of a mammalian voltage-dependent Shaker family K+ channel. Science *309*, 897–903.

Long, S.B., Campbell, E.B., and Mackinnon, R. (2005b). Voltage sensor of Kv1.2: structural basis of electromechanical coupling. Science *309*, 903–908.

Lopez-Barneo, J., Hoshi, T., Heinemann, S.H., and Aldrich, R.W. (1993). Effects of external cations and mutations in the pore region on C-type inactivation of Shaker potassium channels. Receptors Channels *1*, 61–71.

Loukin, S.H., Vaillant, B., Zhou, X.L., Spalding, E.P., Kung, C., and Saimi, Y. (1997). Random mutagenesis reveals a region important for gating of the yeast K+ channel Ykc1. EMBO J. *16*, 4817–4825.

Lukacs, V., Thyagarajan, B., Varnai, P., Balla, A., Balla, T., and Rohacs, T. (2007). Dual regulation of TRPV1 by phosphoinositides. J. Neurosci. *27*, 7070–7080.

Matta, J.A., and Ahern, G.P. (2007). Voltage is a partial activator of rat thermosensitive TRP channels. J. Physiol. *585*, 469–482.

Minor, D.L., Jr., Masseling, S.J., Jan, Y.N., and Jan, L.Y. (1999). Transmembrane structure of an inwardly rectifying potassium channel. Cell *96*, 879–891.

Navarro, B., Kennedy, M.E., Velimirovic, B., Bhat, D., Peterson, A.S., and Clapham, D.E. (1996). Nonselective and G betagamma-insensitive weaver K+ channels. Science *272*, 1950–1953.

Nilius, B. (2007). TRP channels in disease. Biochim. Biophys. Acta *1772*, 805–812.

Oh, U., Hwang, S.W., and Kim, D. (1996). Capsaicin activates a nonselective cation channel in cultured neonatal rat dorsal root ganglion neurons. J. Neurosci. *16*, 1659–1667.

Ou, X., Blount, P., Hoffman, R.J., and Kung, C. (1998). One face of a transmembrane helix is crucial in mechanosensitive channel gating. Proc. Natl. Acad. Sci. USA *95*, 11471–11475.

Peier, A.M., Reeve, A.J., Andersson, D.A., Moqrich, A., Earley, T.J., Hergarden, A.C., Story, G.M., Colley, S., Hogenesch, J.B., McIntyre, P., et al. (2002). A heat-sensitive TRP channel expressed in keratinocytes. Science *296*, 2046–2049.

Prescott, E.D., and Julius, D. (2003). A modular PIP2 binding site as a determinant of capsaicin receptor sensitivity. Science *300*, 1284–1288.

Ryu, S., Liu, B., Yao, J., Fu, Q., and Qin, F. (2007). Uncoupling proton activation of vanilloid receptor TRPV1. J. Neurosci. *27*, 12797–12807.

Sadja, R., Smadja, K., Alagem, N., and Reuveny, E. (2001). Coupling Gbetagamma-dependent activation to channel opening via pore elements in inwardly rectifying potassium channels. Neuron *29*, 669–680.

Serrano, R., and Rodriguez-Navarro, A. (2001). Ion homeostasis during salt stress in plants. Curr. Opin. Cell Biol. *13*, 399–404.

Smith, G.D., Gunthorpe, M.J., Kelsell, R.E., Hayes, P.D., Reilly, P., Facer, P., Wright, J.E., Jerman, J.C., Walhin, J.P., Ooi, L., et al. (2002). TRPV3 is a temperature-sensitive vanilloid receptor-like protein. Nature *418*, 186–190.

Su, Z., Zhou, X., Haynes, W.J., Loukin, S.H., Anishkin, A., Saimi, Y., and Kung, C. (2007). Yeast gain-of-function mutations reveal structure-function relationships conserved among different subfamilies of transient receptor potential channels. Proc. Natl. Acad. Sci. USA *104*, 19607–19612.

Tombola, F., Pathak, M.M., and Isacoff, E.Y. (2006). How does voltage open an ion channel? Annu. Rev. Cell Dev. Biol. *22*, 23–52.

Tominaga, M., Caterina, M.J., Malmberg, A.B., Rosen, T.A., Gilbert, H., Skinner, K., Raumann, B.E., Basbaum, A.I., and Julius, D. (1998). The cloned capsaicin receptor integrates multiple pain-producing stimuli. Neuron *21*, 531–543.

Voets, T., Prenen, J., Vriens, J., Watanabe, H., Janssens, A., Wissenbach, U., Bodding, M., Droogmans, G., and Nilius, B. (2002). Molecular determinants of permeation through the cation channel TRPV4. J. Biol. Chem. *277*, 33704–33710.

Voets, T., Janssens, A., Droogmans, G., and Nilius, B. (2004). Outer pore architecture of a Ca2+-selective TRP channel. J. Biol. Chem. *279*, 15223–15230.

Winter, J. (1987). Characterization of capsaicin-sensitive neurones in adult rat dorsal root ganglion cultures. Neurosci. Lett. *80*, 134–140.

Wood, J.N., Winter, J., James, I.F., Rang, H.P., Yeats, J., and Bevan, S. (1988). Capsaicin-induced ion fluxes in dorsal root ganglion cells in culture. J. Neurosci. *8*, 3208–3220.

Xiao, R., Tian, J., Tang, J., and Zhu, M.X. (2007). The TRPV3 mutation associated with the hairless phenotype in rodents is constitutively active. Cell Calcium *43*, 334–343.

Xu, H., Ramsey, I.S., Kotecha, S.A., Moran, M.M., Chong, J.A., Lawson, D., Ge, P., Lilly, J., Silos-Santiago, I., Xie, Y., et al. (2002). TRPV3 is a calcium-permeable temperature-sensitive cation channel. Nature *418*, 181–186.

Xu, H., Delling, M., Li, L., Dong, X., and Clapham, D.E. (2007). Activating mutation in a mucolipin transient receptor potential channel leads to melanocyte loss in varitint-waddler mice. Proc. Natl. Acad. Sci. USA *104*, 18321–18326.

Yeh, B.I., Kim, Y.K., Jabbar, W., and Huang, C.L. (2005). Conformational changes of pore helix coupled to gating of TRPV5 by protons. EMBO J. *24*, 3224–3234.

Yellen, G. (1998). The moving parts of voltage-gated ion channels. Q. Rev. Biophys. *31*, 239–295.

Yi, B.A., Lin, Y.F., Jan, Y.N., and Jan, L.Y. (2001). Yeast screen for constitutively active mutant G protein-activated potassium channels. Neuron *29*, 657–667.

Zhou, Y., Morais-Cabral, J.H., Kaufman, A., and MacKinnon, R. (2001). Chemistry of ion coordination and hydration revealed by a K+ channel-Fab complex at 2.0 A resolution. Nature *414*, 43–48.

Zhou, X., Su, Z., Anishkin, A., Haynes, W.J., Friske, E.M., Loukin, S.H., Kung, C., and Saimi, Y. (2007). Yeast screens show aromatic residues at the end of the sixth helix anchor transient receptor potential channel gate. Proc. Natl. Acad. Sci. USA *104*, 15555–15559.

Neuron, Volume *58*

Supplemental Data

A Yeast Genetic Screen Reveals a Critical Role for the Pore Helix Domain in TRP Channel Gating

Benjamin R. Myers, Christopher J. Bohlen, and David Julius

Figure S1 Mutations recovered in the TRPV1 N-terminus affect channel activation

(**A**) Yeast growth assay and (**B**) TEVC analysis of basal currents for alanine or glutamate substitutions of N-terminal K155 and K160 residues. Yeast growth assays and electrophysiological experiments were performed as outlined in figures 1 and 3, respectively.

A

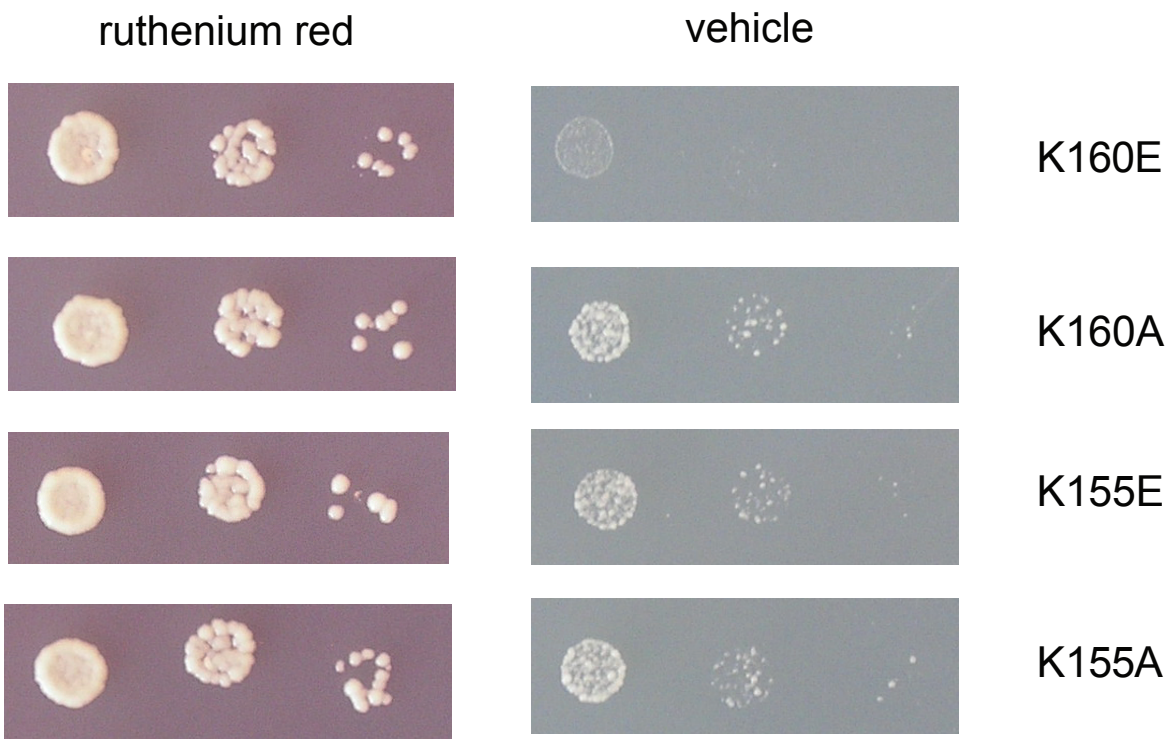

B

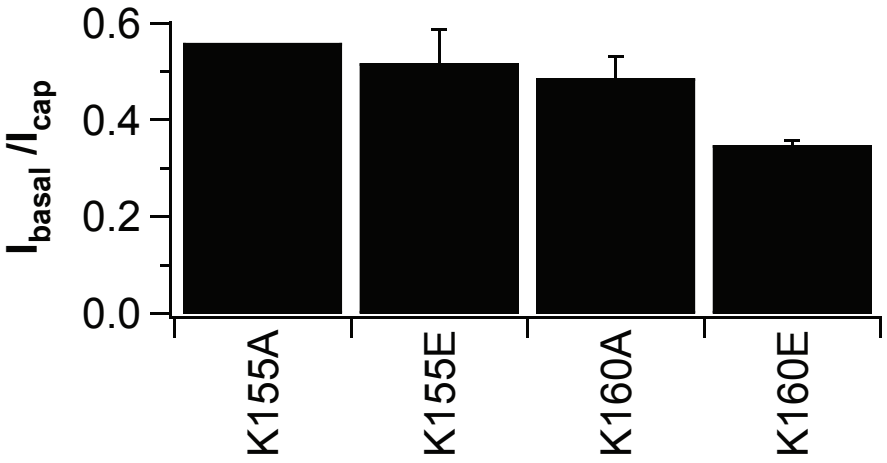

Myers et al, Figure S1

Figure S2 The F640L mutation does not affect TRPV1 single channel conductance or ion permeation properties

Single-channel currents were recorded in the cell-attached configuration from HEK293 cells transfected with wild type TRPV1 (**A**) or the F640L mutant (**B**). The pipette solution contained 1 μM capsaicin. Recording were performed at pipette potentials of +60 to +100 mV and the slope conductance was calculated by linear regression, yielding values of 155.3 ± 8.1 pS vs. 147.0 ± 5.6 pS for wild type and F640L, respectively (n = 3). Single channel i-V relations were determined by ensemble averaging of leak-subtracted voltage ramp traces from excised inside-out patches and normalized to the maximal current at +70 mV. The pipette solution contained 1 μM capsaicin. (**C**) Relative ion permeability ratios of capsaicin-evoked currents from wild type or F640L mutant channels were estimated from reversal potential shifts in whole cell patch clamp recordings of transfected HEK293 cells, revealing no significant differences.

A

wild type
TRPV1

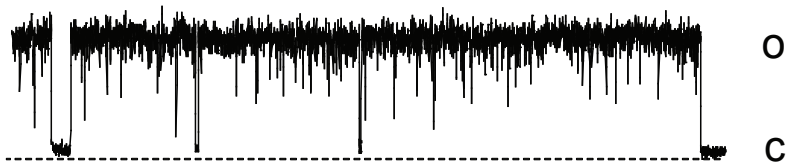

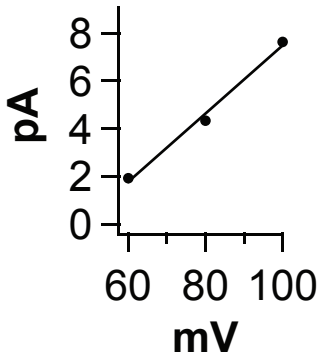

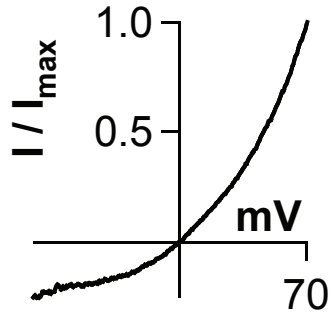

B

F640L

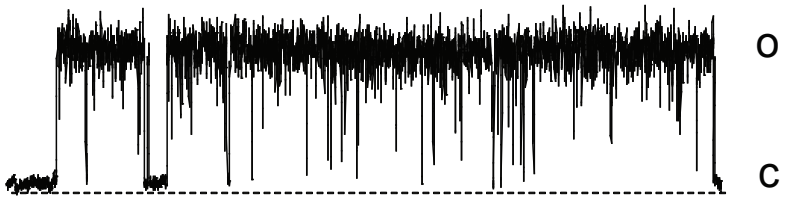

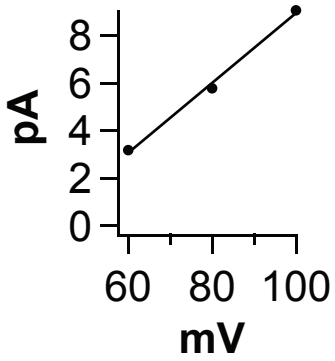

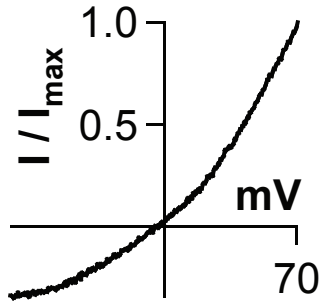

3 pA

150 ms

C

Channel	P_K / P_{Na}	P_{Ca} / P_{Na}
wild type TRPV1	1.22 ± 0.08	4.89 ± 2.25
F640L	1.13 ± 0.12	6.28 ± 0.80

Myers et al, Figure S2

Table S1. Summary of Yeast Screens of Mutant Libraries.

Mutant Library	Library Complexity	Average Number of Amino Acid Mutations Per Clone	Number of Clones Screened	Number Scored as Gain-of-function	Hit Rate
N-terminus	6.8×10^4	1.67	1.3×10^4	20	0.15%
C-terminus	1.8×10^5	1.67	3.3×10^4	26	0.08%
Pore Helix	1.5×10^4	1.14	1.5×10^4	26	0.17%

Table S2. Summary of yeast toxicity and electrophysiological properties of TRPV1 mutants recovered from the genetic screen.

cDNA	Number of Times Recovered	Yeast Toxicity	I_{basal} / I_{cap}	$I_{pH\ 6.4}$ / I_{cap}	Constitutive Activity?[1,2]	Potentiation?[2]
C73S	1	strong	0.080 ± 0.003	0.007 ± 0.003		
I75F	1	weak	-0.010 ± 0.034	0.020 ± 0.010		
I76T	1	weak	-0.060 ± 0.041	0.022 ± 0.018		
V78G	1	weak	0.000 ± 0.013	0.014 ± 0.008		
K155E	3	weak	0.320 ± 0.052	0.248 ± 0.042	**YES**	**YES**
K160E	4	strong	0.427 ± 0.033	0.423 ± 0.008	**YES**	**YES**
H166R	1	weak	0.133 ± 0.011	0.276 ± 0.015		**YES**
N310D	2	weak	-0.020 ± 0.031	0.024 ± 0.015		
S343G	1	weak	0.050 ± 0.033	0.008 ± 0.013		
S343R	1	strong	0.020 ± 0.026	0.025 ± 0.019		
A350T	2	strong	0.000 ± 0.022	0.018 ± 0.018		
I352N	1	weak	0.040 ± 0.090	0.136 ± 0.070		**YES**
I352T	1	weak	0.090 ± 0.015	0.114 ± 0.024		**YES**
Q560R	1	weak	0.070 ± 0.035	0.128 ± 0.035		**YES**
Q561R	2	strong	0.070 ± 0.022	0.025 ± 0.001		
M581T	2	strong	0.208 ± 0.021	0.270 ± 0.019	**YES**	**YES**
M609T	1	strong	0.030 ± 0.021	0.012 ± 0.012		
M609V	1	weak	-0.020 ± 0.048	0.025 ± 0.012		
F640L	1	strong	0.516 ± 0.025	0.016 ± 0.015	**YES**	
N652D	1	strong	0.070 ± 0.009	0.088 ± 0.027		**YES**
L673I*	1	strong	0.070 ± 0.022	0.011 ± 0.005		
E684G	5	strong	0.109 ± 0.002	0.115 ± 0.013		**YES**
E684V	4	strong	0.090 ± 0.014	0.031 ± 0.011		**YES**
I689V	1	weak	0.050 ± 0.014	0.006 ± 0.006		
K710R	1	strong	-0.030 ± 0.031	0.014 ± 0.007		
F742S	1	strong	0.040 ± 0.003	0.031 ± 0.014		
W787R	1	strong	-0.030 ± 0.011	0.013 ± 0.003		
L792P	1	weak	0.050 ± 0.008	0.094 ± 0.013		**YES**
L796P	1	strong	-0.010 ± 0.010	0.010 ± 0.011		
L796V	1	weak	0.020 ± 0.010	0.023 ± 0.012		
WT			0.000 ± 0.020	0.015 ± 0.003		

[1] Mutants showing $I_{basal}/I_{cap} \geq 15\%$ were classified as constitutively active.
[2] For mutants scoring positive in each category, $p \leq 0.05$ compared to wild-type TRPV1 (Student's t-test).
* For L673I, responses were normalized to 100 μM capsaicin.